Surface heterogeneity in Au-Ag nanoparticles probed by hyper-Rayleigh scattering

Isabelle Russier-Antoine,* Guillaume Bachelier, Virginie Sablonière, Julien Duboisset, Emmanuel Benichou, Christian Jonin, Franck Bertorelle, and Pierre-François Brevet

Laboratoire de Spectrométrie Ionique et Moléculaire, UMR CNRS 5579, Université Claude Bernard Lyon 1, Bâtiment Alfred Kastler, 43 Boulevard du 11 Novembre 1918, 69622 Villeurbanne Cedex, France

(Received 13 March 2008; published 21 July 2008)

Aqueous solutions of alloyed gold-silver nanoparticles, the diameter of which ranged between 15 and 50 nm, were prepared with varying molar fractions. The UV-Visible photoabsorption spectra for all solutions were dominated by a single surface-plasmon resonance, the wavelength of which was found to change linearly with the molar fraction. A model, in agreement with these findings, was then derived to compute a dielectric constant for the different alloyed gold-silver nanoparticles based on a weighted function of the pure gold and pure silver dielectric constants. Hyper-Rayleigh scattering measurements were performed for these alloyed metallic nanoparticles solution to determine their quadratic hyperpolarizability. Theses values, once corrected for their size and local-field factors dependencies, are found to be larger than the corresponding values for the pure gold and pure silver nanoparticles. This is attributed to the atomic surface heterogeneity of these alloyed gold-silver particles, underlining the potential of the method to investigate the surface of nanometer scale metallic particles, especially in catalysis. This atomic surface heterogeneity is assigned to the differences between the Au and Ag atoms in their interband transitions since their intraband parameters are very similar.

DOI: 10.1103/PhysRevB.78.035436 PACS number(s): 78.67.Bf, 42.65.−k, 68.05.−n, 73.22.−f

I. INTRODUCTION

Over the last decade, the interest in small metal particles, especially gold and silver metallic particles, has dramatically increased, mostly because of their unique optical and electronic properties. These properties are dominated by the collective excitation of the conduction-band electrons known as the surface-plasmon resonance (SPR).[1] These properties are often investigated by optical methods, principally linear optical methods, but more recently nonlinear optical methods have been successively used. This is due to the large enhancements expected for the electromagnetic fields through the SPR.[2] For particles dispersed in a liquid solution, a method of choice is hyper-Rayleigh scattering (HRS), namely the scattering of the light produced by the conversion of two photons at a fundamental frequency into one photon at the harmonic frequency.[3,4] SPR enhancement can be obtained at the fundamental or the harmonic frequency yielding more versatility although SPR enhancement at the fundamental frequency is usually avoided in order to preserve the sample solution from degradation. As a result, large magnitudes for the quadratic hyperpolarizability tensor of silver and gold nanoparticles have been reported recently.[5–8] However, for perfectly spherical metallic nanoparticles that are small compared to the wavelength of light, no HRS signal intensity should be collected owing to the centrosymmetry of both the material crystal structure and the shape of the particle within the electric dipole approximation.[9–13] This paradox has been solved recently for metallic gold and silver particles.[14–16] Indeed, it has been demonstrated that the frequency conversion process finds its origin at the particle surface and is due to the shape of the particles, which is not perfectly spherical. As a consequence, the total HRS response is of pure electric dipole nature for the smallest particles, but for larger particles, retardation effects in the electromagnetic fields must be considered. Hence, in this case, a non-negligible quadrupolar contribution is observed, which may even dominate for the largest particles. It has therefore been shown that it could be interesting to introduce a weighting parameter to give a quantitative figure for the weight of the dipole and the quadrupole contributions.[14] Furthermore, the role of the enhancement of the HRS intensity through the SPR excitation on the weight of the electric and quadrupolar contributions has also been discussed.[17,18] Theses features have been observed on pure metal particles and it is therefore of interest to investigate the role of alloying, e.g., when a silver atom is replaced by a gold atom, or vice versa.

In the present work, the continuous transition from pure silver to pure gold nanoparticles is investigated using aqueous suspensions of alloyed gold-silver nanoparticles with varying molar fraction from the point of view of their linear and nonlinear optical properties. The linear optical properties are investigated and are compared with the results obtained within the Mie theory using dielectric functions computed from experimental data of both silver and gold bulk dielectric functions.[19,20] The value of the quadratic hyperpolarizability tensor magnitude, corrected by its local-field factors and its size dependences, is also reported and discussed in connection with the particles surface heterogeneity and with the continuous shift of the intraband transitions threshold with composition.

II. EXPERIMENT SECTION

Particles synthesis: Hydrogen tetrachloroaurate (III) hydrate, silver nitrate, trisodium citrate dehydrate, and sodium borohydride were all obtained from Sigma-Aldrich. Milli-Q water with 18.2 $M\Omega/cm$ resistivity was used in all preparations. All glassware and magnetic stirring bars were cleaned in aqua regia. Gold nanoparticles were prepared following the standard method described by Turkevich.[21] 49 mL of a 2.5 mM $HAuCl_4$ aqueous solution was brought to ebullition

TABLE I. x is the gold molar fraction ($Au_xAg_{(1-x)}$), λ_{max} is the maximum position of the UV-Vis spectrum, D is the diameter of the nanoparticle, $\sqrt{\langle\beta^2\rangle}$ is the quadratic hyperpolarizability value, $\sqrt{\langle(\beta^V)^2\rangle}$ is the quadratic hyperpolarizability tensor magnitude in vertically polarized second-harmonic intensity configuration, $f(\omega)$ is the local-field factor correction, $\sqrt{\langle(\beta_0^V)^2\rangle}$ is the reduced hyperpolarizability defined in Eq. (6), and ζ^V is the weighting parameter used to estimate the relative magnitude of the dipolar and quadrupolar contributions.

x	λ_{max}/nm	D/nm	$\sqrt{\langle\beta^2\rangle}/10^{-27}$ esu	$f(\omega)/10^{-3}$	$\sqrt{\langle(\beta^V)^2\rangle}/10^{-27}$ esu	$\sqrt{\langle(\beta_0^V)^2\rangle}/10^{-22}$ esu	ζ^V
1	519	16	90(2)	0.480	80(2)	400	0.04
0.8	503	32	510(4)	0.423	365(4)	530	0.28
0.7	493	38	455(13)	0.409	310(10)	330	0.39
0.6	481	40	710(15)	0.401	535(11)	525	0.31
0.5	473	47	1060(11)	0.424	675(6)	455	0.45
0.4	445	43	1050(9)	0.541	725(6)	455	0.29
0.3	435	44	1270(11)	0.517	810(6)	325	0.43
0.2	429	30	560(9)	1.47	400(6)	190	0.19
0	402	17	340(8)	2.86	260(6)	200	0.11

under vigorous magnetic stirring. Then 1 mL of a 2.5% citrate solution was added and the final solution was heated under reflux for 30 min. Gold-silver alloyed particles were prepared in the same way by substituting a fixed quantity of tetrachloroaurate by the same amount of silver nitrate. Alloyed particles with gold molar fractions of 0.8, 0.7, 0.6, 0.5, 0.4, 0.3, and 0.2 were made this way. The synthesis of the pure silver nanoparticles was slightly changed with the addition of 25 μL of a 0.01 M solution of $NaBH_4$ after the introduction of sodium citrate.

Particle characterization: Dynamic light scattering (DLS) was performed on a Malvern Zetasiser Nano using the noninvasive back scattering (NIBS) technology to allow measurements with samples with little or no dilution (the position of the detector was set at 173° relative to the laser source). The hydrodynamic mean diameter of the particles was determined using the software provided by Malvern. All measurements were performed at 298 K with a continuous laser running at 633 nm with polystyrene cells. The UV-Visible photoabsorption spectra were obtained using a compact spectrophotometer (USB 2000, Ocean Optics). All size distribution has a width less than 15%. The particles diameters are reported in Table I. It was noticed that the diameter of the mixed metal particles were always larger than that of the pure metal ones. This is attributed to slight differences in the reaction path for the two metal ions.

HRS measurements: The light source for the present HRS experiments was a mode-locked femtosecond Ti:sapphire laser delivering at the fundamental wavelength of 790 nm pulses with a duration of about 180 fs at a repetition rate of 76 MHz. After passing through a low-pass filter to remove any unwanted harmonic light generated prior to the cell, the fundamental beam of about 900 mW was focused by a microscope objective into a 1×1 cm^2 spectrophotometric cell containing the aqueous solution of the metallic particles. The HRS light was collected at an angle of 90° from the incident direction by a 2.5 cm focal length lens. The second-harmonic light was separated from its linear counterpart by a high-pass filter and a monochromator positioned on the second-harmonic wavelength. The HRS light was then detected with a cooled photomultiplier and a photon counter. The fundamental beam was chopped at about 130 Hz to enable a gated photon counting mode allowing automatic subtraction of the noise level. The fundamental input beam was linearly polarized and the input angle of polarization γ was selected with a rotating half-wave plate.

III. LINEAR OPTICAL PROPERTIES

A. UV-visible absorption spectra

The optical properties of metal particles are dominated by the SPR, the collective oscillation of the conduction electrons upon interaction with an incoming electromagnetic field.[1] For some metals, such as Cu, Ag, Au, or the alkali metals, the SPR frequency lies within the visible range for nanosized particles and is responsible for the intense colors observed with colloidal dispersions.[22] When two different metals are mixed within a single particle, the resulting optical properties arise from a combined contribution of both metals, and the spatial distribution of the metal atoms within the particle is of fundamental importance. Bimetallic nanoparticles with a core-shell morphology have been studied in the past and their linear and nonlinear optical properties were compared with calculations based on the Mie theory.[23–29] In the case of bimetallic alloyed nanoparticles, the wavelength of the SPR was found to change in a linear way between that for the pure silver and that of the pure gold particles as a function of the molar fractions of the metals.[30,31] This feature allows an easy way to tailor the optical properties of metallic nanoparticles. Figure 1 shows the UV-visible photoabsorption spectra for the alloyed gold-silver particles in aqueous suspensions studied in the present work. As expected, the SPR wavelength varies linearly between 400 nm for the pure silver particles and 520 nm for the pure gold particles in agreement with the previous works. The formation of aqueous suspensions of alloyed nanoparticles rather than aqueous mixtures of gold and silver nanoparticles is indicated by the

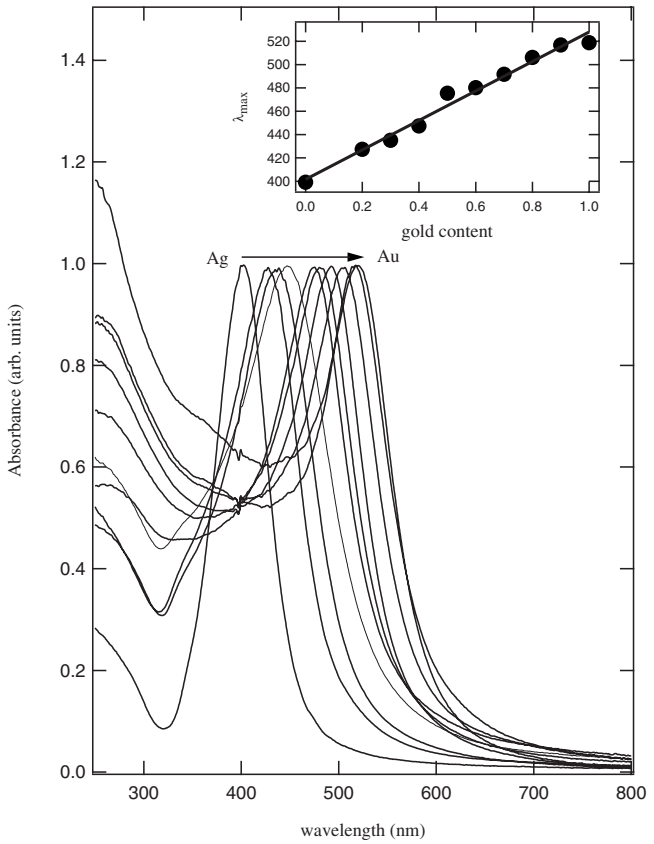

FIG. 1. Normalized UV-visible spectra of Au-Ag alloy nanoparticles with varying composition. Insert: location of the maximum of the SP resonance as a function of the gold content.

presence of a single well-defined SPR band in the spectra.

B. Dielectric constants of the alloyed gold-silver nanoparticles

Absorption and scattering of light by metal nanoparticles is well described with the well-known Mie theory using, as input parameters, the wavelength dependent complex dielectric functions of the bulk materials.[32] Experimental data are available for Au-Ag alloys between about 2.5 and 4.5 eV,[33] but this energy range lies above the excitation energy used in the present experiments, namely, a fundamental photon energy of 1.57 eV. Therefore, the dielectric functions for the Au-Ag nanoparticles had to be extrapolated from the existing data. In the model developed by Gaudry *et al.*,[34] the dielectric functions were deduced from the pure gold and silver bulk properties where the interband threshold energy $\omega^{ib}_{\text{Au-Ag}}$ of the Au-Ag alloyed particles is assumed to scale linearly with the gold molar fraction x:

$$\omega^{ib}_{\text{Au-Ag}}(x) = x\omega^{ib}_{\text{Au}} + (1-x)\omega^{ib}_{\text{Ag}}, \tag{1}$$

where ω^{ib}_{Au} and ω^{ib}_{Ag} are the interband threshold energies for gold and silver, respectively. The imaginary part of the dielectric function, corresponding to the interband transitions, was then computed from the data for pure gold and pure silver using the following expression:[34]

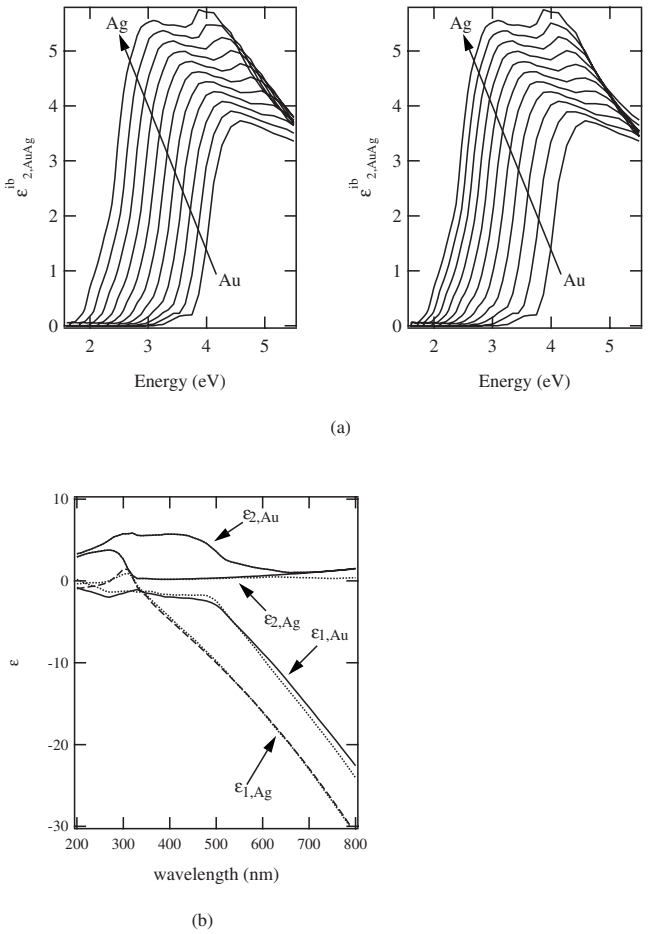

FIG. 2. (a) Interband contribution to the imaginary part of the dielectric constant for gold molar fraction ranging from zero to one as obtained with a linear dependence of the interband threshold energy (left panel) and of the wavelength (right panel). (b) Dielectric functions of gold and silver, ε_2 is the imaginary part of the dielectric functions used in the model (full lines) and ε_1 is the real part of the dielectric functions deduced from the Kramers-Kronig analysis (full line for gold, dashed line for silver). The dotted lines correspond to data from Johnson and Christy.

$$\text{Im}[\varepsilon^{ib}_{\text{Au-Ag}}(x, \omega^{ib}_{\text{Au-Ag}}(x) + \omega')] = x\,\text{Im}[\varepsilon^{ib}_{\text{Au}}(\omega^{ib}_{\text{Au}} + \omega')] + (1-x)\text{Im}[\varepsilon^{ib}_{\text{Ag}}(\omega^{ib}_{\text{Ag}} + \omega')], \tag{2}$$

where $\varepsilon^{ib}_{\text{Au}}$ and $\varepsilon^{ib}_{\text{Ag}}$ are the interband dielectric functions deduced from the experimental data given by Johnson and Christy,[19] subtracting the Drude contribution corresponding to the s conduction electrons.[35] The results are given in Fig. 2(a) left panel. As explained in the work of Gaudry *et al.*,[34] one obtains a smooth evolution of the imaginary part of the interband dielectric function starting from that of pure gold to that of pure silver, in qualitative agreement with the experimental data reported by Nilsson.[36] The real part of the interband dielectric functions were then computed using the Kramers-Kronig relations in the energy range 0–400 eV using the experimental data of Palik[20] to extend the data of Johnson and Christy for pure gold and silver above 6.6 eV.

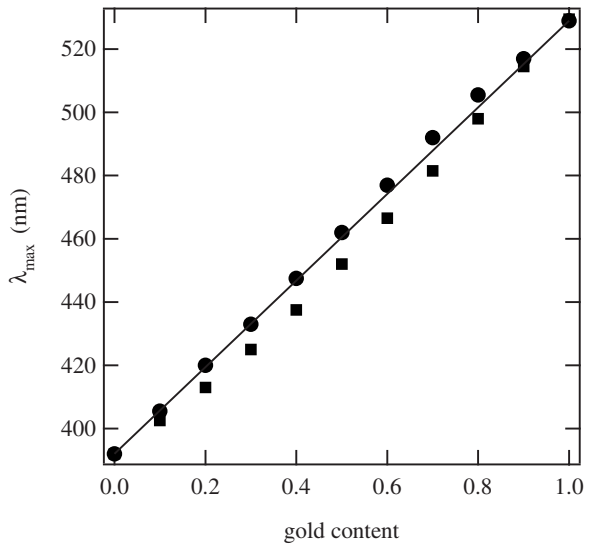

FIG. 3. Location of the maximum of the SPR as a function of gold content obtained with the Mie theory using Eq. (1) (squares) or Eq. (3) (circles). The line corresponds to a linear evolution from the pure silver to the pure gold case.

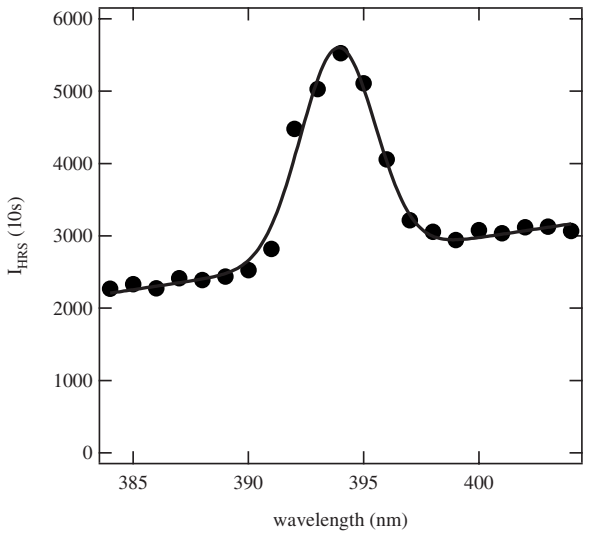

FIG. 4. HRS line for the $Au_{0.6}Ag_{0.4}$ alloyed nanoparticle for a fundamental wavelength of 788 nm. Circles are experimental points and solid line is a fit of the experimental data.

Note that the imaginary part of the interband dielectric functions was set to zero below $\omega^{ib}_{\text{Au-Ag}}(x)$. The results obtained for pure gold and silver are shown on Fig. 2(b). The original experimental data of Johnson and Christy are also reported for comparison. The parameter of the Drude contribution to the dielectric functions was iteratively adjusted to give the best agreement in the 400–520 nm range where the SPR is observed in the Au-Ag alloy nanoparticles (see Fig. 1).

At this stage, the absorption and scattering cross sections for the alloy nanoparticles were computed using Mie theory and the maximum of the SPR plotted as a function of the gold molar fraction (see Fig. 3). As a matter of fact, one does not obtain a linear shift of the SPR wavelength with the molar fraction as observed in Fig. 1. The origin of this discrepancy lies in the expression of the interband energy threshold assumed to follow Eq. (1). However, if a linear shift of the interband threshold wavelength is used instead of the interband threshold energy, namely, if the following equation is used instead of Eq. (1):

$$\lambda^{ib}_{\text{Au-Ag}}(x) = x\lambda^{ib}_{\text{Au}} + (1-x)\lambda^{ib}_{\text{Ag}}, \tag{3}$$

then one recovers the linear dependence of the SPR as a function of the gold content, as observed experimentally. Furthermore, the evolution of the imaginary part of the interband dielectric functions with the gold molar fraction, see Fig. 2(a) right panel, is in better agreement with the experimental data of Nilsson.[36] Hence, hereafter the dielectric functions computed using Eq. (3) are used in the remainder of this work.[35]

IV. NONLINEAR OPTICAL PROPERTIES

A. Hyperpolarizability measurements

In these experiments where the HRS intensity is collected, the monochromaticity of the second-harmonic light generated was always assessed to prevent any spurious contributions from luminescence. To this end, a spectrum was recorded for a solution of $Au_{0.6}Ag_{0.4}$ nanoparticles for a fixed incident fundamental wavelength, see Fig. 4. This experimental procedure is necessary to ensure that the observed process is indeed the conversion of two photons at the fundamental frequency into one photon at the harmonic frequency and to determine the level of luminescence. Luminescence from gold nanoparticles has already been reported in the past and is usually attributed to surface trap states owing to the coating of the particles.[5,37] The observation of a luminescence background at energies higher than the HRS line suggests that the excitation process is at least a three photon process. Experiments were conducted on pure water and citrate solutions to reject any contributions arising from by-products of the particle synthesis. No signal was observed during these measurements. The HRS line for this sample solution is shown in Fig. 4. The solid line is a fit to a Gaussian function for the HRS line superimposed on a linear function of the wavelength to account for the broad luminescence background. This operation can indeed be performed since the two processes, luminescence and HRS, are incoherent. The weight of the luminescence contribution at the harmonic wavelength of 394 nm was as large as 50% of the total signal intensity collected. These results clearly call for a careful analysis of the data in order to truly determine the quadratic hyperpolarizabilities of the Au-Ag alloyed particles. Hereafter, the HRS intensity is always taken as the height of the Gaussian part of the fitting function.

The experiments consisted in the determination of the absolute value of the quadratic hyperpolarizability tensor magnitude for Au-Ag alloyed nanoparticles. The HRS intensity is given by[4]

$$I_{\text{HRS}} = G\langle N_S\beta_S^2 + N\beta^2\rangle I^2, \tag{4}$$

where I is the fundamental intensity, N_S and N, and β_S and β are the number densities and the quadratic hyperpolarizabili-

ties of the solvent and the metallic nanoparticles, respectively. In Eq. (4), the HRS intensity is corrected for self-absorption. G is a general factor embedding all geometrical factors as well as absolute constants. Finally the brackets state that an orientation average is considered owing to the isotropy of the liquid phase. The measurement of the HRS intensity in the absence of particles provides an internal reference for the determination of the absolute values of the first hyperpolarizabilities, since N_S and β_S are known for water. A value of $\beta_S = 0.56 \times 10^{-30}$ esu was used for water.[6] Using successive dilutions of the initial concentrated solutions, the absolute values of the quadratic hyperpolarizability tensor magnitudes, given in terms of $\beta = \sqrt{\langle \beta_{XXX}^2 \rangle + \langle \beta_{ZXX}^2 \rangle}$ where the elements of the hyperpolarizability tensors are assumed within the laboratory frame, were measured for all Au-Ag alloyed particles. The data are reported in Table I. At this stage, these hyperpolarizability values are hardly comparable because they are dramatically affected by the particle size and the SPR enhancements. Nevertheless, the values reported are rather large and are compared well in orders of magnitudes with the one reported for pure gold and pure silver particles in this work and in previous works as well.[15]

B. Size and local-field factor corrections

The dependence of the quadratic hyperpolarizability as a function of the particle size has been studied in detail for gold and silver nanoparticles.[15,17] It was demonstrated in particular that retardation effects of the electromagnetic fields cannot be neglected for particle sizes above about 40 nm. Hence, a similar approach was used in the present work in order to investigate the size dependence of the quadratic hyperpolarizability of the Au-Ag alloyed nanoparticles: polar plots of the HRS intensity as a function of the angle of polarization γ of the linearly polarized fundamental beam were recorded for all alloyed particles. The polar plot obtained for an aqueous suspension of $Au_{0.6}Ag_{0.4}$ alloyed particles is given in Fig. 5. For each polarization angle γ, the luminescence was subtracted following the procedure described above. Experimental data were then adjusted with the following expression of the HRS intensity:

$$I_{HRS}^{\Gamma} = a^{\Gamma} \cos^4 \gamma + b^{\Gamma} \cos^2 \gamma \sin^2 \gamma + c^{\Gamma} \sin^4 \gamma, \qquad (5)$$

where a^{Γ}, b^{Γ}, and c^{Γ} are fitting parameters depending on the polarization of the HRS signal, Γ is either vertical ($\Gamma = V$) or horizontal ($\Gamma = H$). Equation (5) is similar to Eq. (4) but the polarization angle γ is made explicit now. The relative magnitude of the dipolar and quadrupolar contributions were then estimated using the weighting parameter $\zeta^V = |(b^V - a^V - c^V)/b^V|$ as used previously.[15,17] This latter parameter ranges from zero for a pure dipolar response to unity for a pure quadrupolar one. Larger values for this parameter were always found for pure silver nanoparticles as compared to pure gold nanoparticles. This is in agreement with the larger retardation effects observed in linear optics for silver nanoparticles.[38] It is also important to assess whether the origin of the second harmonic response from Au-Ag alloyed metallic particles is similar to that of the pure gold and silver particles. To investigate this question, polar plots were recorded for all Au-Ag alloyed solutions. The corresponding ζ^V values obtained after fitting with Eq. (5) are reported in Table I and Fig. 6 as a function of the gold molar fraction. Despite the rather large data fluctuations, a clear increase in the weighting parameter is observed for intermediate compositions. However, one cannot conclude here whether the origin arises from the nanoparticles size or from the gold molar fraction. To go further in the analysis, the ζ^V values for pure silver and gold nanoparticles were extrapolated using previous data[15,17] for the particle sizes investigated in the present

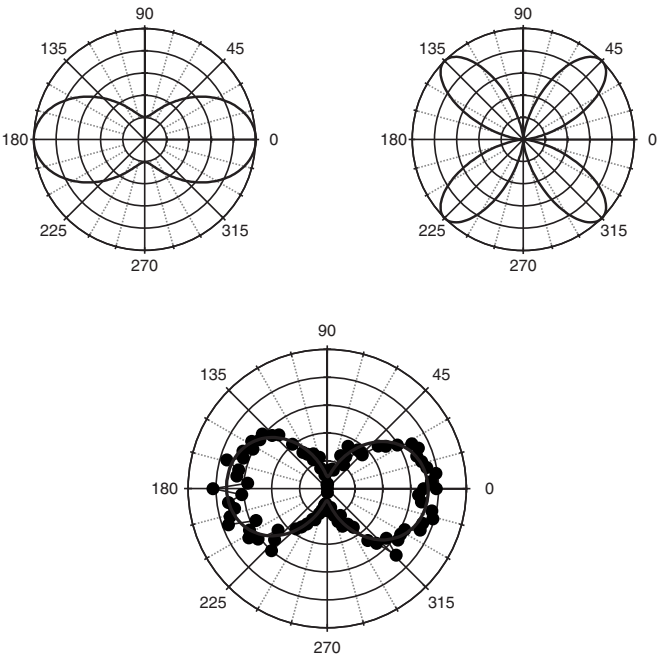

FIG. 5. Polar plot of the HRS intensity as a function of the incoming fundamental beam polarization angle: (filled circles) experimental points for an aqueous suspension of $Au_{0.6}Ag_{0.4}$ alloyed particles and (solid) fit to the experimental data points using Eq. (5). Left insert: polar plot of a pure dipolar response, right insert: polar plot of a pure quadrupolar response.

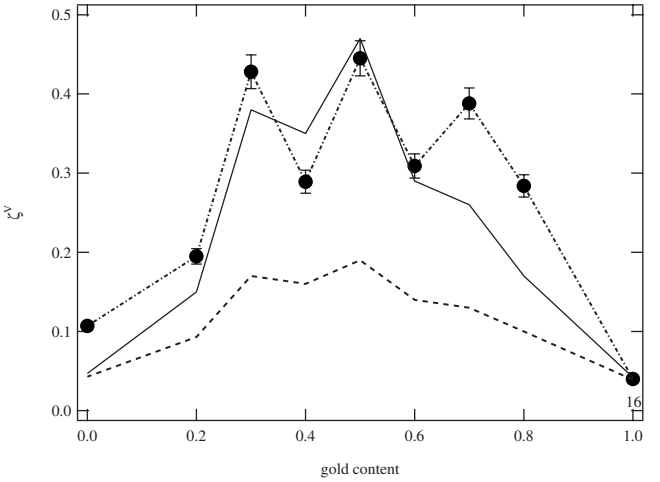

FIG. 6. Plot of the ζ^V parameter (circle) as a function of gold content. The full and dashed lines correspond to extrapolated data from pure silver and pure gold nanoparticles, respectively.

work. The corresponding data are reported in Fig. 6 for comparison. As previously discussed, the weighting parameter is always larger for pure silver nanoparticles than for pure gold ones but in both cases it reaches a maximum for intermediate molar fractions, see Table I. A good qualitative agreement is observed between the ζ^V values measured for the Au-Ag alloyed particles and the ones recalculated using that of the pure silver particles and taking into account the size of the alloyed particles. At low gold molar fractions, it appears that the two values for the ζ^V parameter are very similar. This is, however, not the case for large gold molar fractions where the weighting parameter significantly deviates from the extrapolated values recalculated from the ζ^V parameter of the pure gold nanoparticles. As a matter of fact, the weighting parameters measured for the Au-Ag alloyed nanoparticles are always closer to the values extrapolated from the ζ^V parameter of pure silver particles than of pure gold particles. Small amounts of silver in the particles therefore play a major role in the alloyed nanoparticles, inducing larger values for the ζ^V parameter.

In order to facilitate the particle size and the local-field factor corrections to the quadratic hyperpolarizability β, the experiments were performed with a vertically polarized fundamental beam, that is with $\gamma=0°$, a polarization configuration where no signal is expected from the quadrupolar response at the emission stage (see inset of Fig. 5). Hence, only the radiated dipolar response is selected in this configuration. Furthermore, only the vertically polarized second-harmonic intensity was recorded. The corresponding quadratic hyperpolarizability tensor magnitude β^V, see Table I, was therefore corrected using the purely dipolar expression,

$$\sqrt{\langle \beta^{V^2} \rangle} = \frac{(ka)^2}{|\varepsilon_{\text{Au-Ag}}(\Omega) + 2\varepsilon_s| \cdot |\varepsilon_{\text{Au-Ag}}(\omega) + 2\varepsilon_s|^2} \sqrt{\langle \beta_0^{V^2} \rangle}, \tag{6}$$

where $(ka)^2$ accounts for the surface dependence of the quadratic susceptibility observed for dipolar response of gold and silver nanoparticles. Here k is the fundamental wave vector and a is the radius of the particles taken as the hydrodynamic radius measured by DLS. The difference between the latter and the real diameter was found negligible. The factors $|\varepsilon_{\text{Au-Ag}}(\omega)+2\varepsilon_s|^{-1}$ and $|\varepsilon_{\text{Au-Ag}}(\Omega)+2\varepsilon_s|^{-1}$ are the local-field factors at the fundamental and harmonic frequencies (ω and $\Omega=2\omega$, respectively), arising from the field enhancement in the metal particles[12,18] where ε_s is the dielectric constant of the solvent and $\varepsilon_{\text{Au-Ag}}$ that of the different Au-Ag alloyed nanoparticles as obtained by the model discussed above. The overall local-field factors are given in Table I. At the harmonic wavelength of 394 nm, large enhancements, i.e., large local-field factors, are expected for the nanoparticles with large silver content owing to the location of their SPR. At the fundamental wavelength of 788 nm, Fig. 2(b) shows that $\varepsilon_{1\text{Au}}$ and $\varepsilon_{1\text{Ag}}$ are significantly different so that the quadratic term plays a non-negligible role in the overall enhancement factor, leading finally to the increase in the local-field factor for large gold molar fractions.

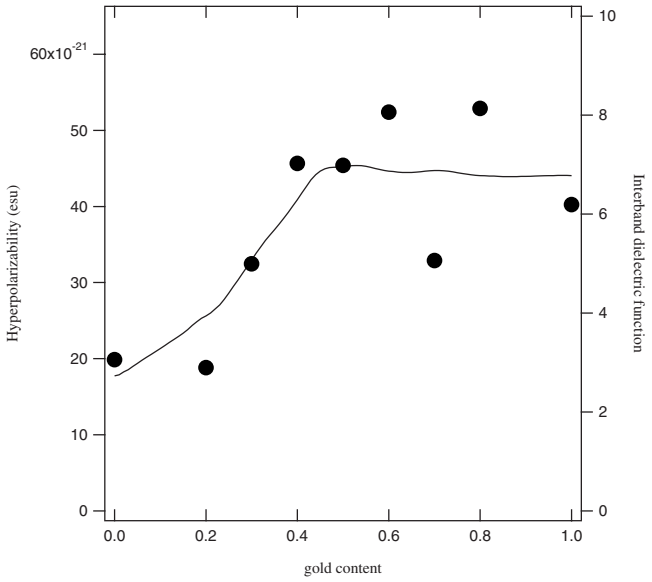

FIG. 7. Corrected hyperpolarizability values as a function of gold content (circles) and modulus of the interband transitions contributions to the dielectric function (solid line).

C. Alloying effect on the second harmonic response

The quadratic hyperpolarizability values corrected for the particle sizes and the field factors are given in Table I and reported in Fig. 7 as a function of gold molar fraction. For pure gold and pure silver particles, the hyperpolarizability values are in good agreement with previous measurements.[15] For Au-Ag alloyed nanoparticles, the corrected hyperpolarizability values are larger than the values obtained assuming a linear dependence of the hyperpolarizability with the metal composition. Similarly to the weighting parameter ζ^V, the deviation from the expected results is larger for large gold molar fractions than for the smaller ones. This deviation could arise from the retardation effects associated with the fundamental incident beam. Indeed, in the polarization configuration used, the dipolar contribution is indeed composed of a pure electric dipole contribution and a contribution due to the fundamental field retardation effects. This contribution cannot be disentangled in the present configuration. However, retardation effects are larger for pure silver particles than for pure gold nanoparticles and therefore are not likely to explain the observed deviation of the hyperpolarizability from a linear behavior with respect to the gold molar fraction. Since both the size and the local-field factors were taken into account, the origin of this behavior is attributed to another contribution of the nonlinear polarization source, namely, the atomic surface inhomogeneity, that is a nonuniform distribution of the metal atoms at the particle surface. Such a nonuniform distribution within the volume of the particle would locally break down the inversion symmetry, with noncentrosymmetrical crystallographic sites due to the presence of atoms of different natures, and thus allows a true electric dipole bulk contribution to the quadratic hyperpolarizability. However, the random distribution of these noncentrosymmetrical sites should cancel their respective contributions. Hence, it is concluded that the atomic heterogeneity

only dominates at the surface where it becomes another contribution to the quadratic hyperpolarizability of the alloyed metallic particles.

It is finally interesting to compare the behavior of the interband transitions contribution to the dielectric functions of the alloyed particles with that of the corrected hyperpolarizability as a function of the gold molar fraction. Indeed, gold and silver atoms have very similar properties with respect to their free electrons. Consequently, the corrected quadratic hyperpolarizability should not be severely affected by the substitution of gold atoms by silver ones and vice versa if one considers the intraband contributions only. On the opposite, the interband transitions are continuously shifted in energy with the gold molar fraction as shown in the previous section. Therefore, one may expect that the difference between the gold and the silver atoms is exhibited through the interband transitions. In order to evidence a possible link between the interband transitions and the corrected hyperpolarizability magnitude, the modulus of the interband dielectric function, as calculated from the model developed above, is also reported in Fig. 7 for comparison. Both the corrected hyperpolarizability and the interband dielectric function present the same behavior as a function of the gold molar fraction suggesting a close correlation that is yet to be fully revealed.

V. CONCLUSIONS

Aqueous solutions of gold-silver alloyed nanoparticles with varying compositions were prepared. The UV-visible absorption spectra showed a linear blueshift of the location of the maximum of the surface-plasmon resonance with increasing silver content. To correctly account for this behavior, a model is derived to compute the dielectric functions of the alloyed particles starting from that of the pure metals. Hyper-Rayleigh scattering measurements were then performed. The hyperpolarizability values obtained are as large as that reported previously for pure gold and pure silver nanoparticles. After corrections for the particle sizes and the local-field factors, the corrected hyperpolarizability values are found systematically larger for the alloyed particles than for the pure gold and pure silver ones. The origin of this behavior is attributed to a nonuniform distribution of the metal atoms at the particle surface. Interestingly, the interband transitions contribution to the dielectric function presents a behavior very similar to that of the corrected hyperpolarizability with the gold molar fraction. It therefore appears that this atomic surface inhomogeneity for gold-silver alloyed particles essentially stems from the differences between these two atoms in their interband transitions since their intraband parameters are very similar.

*Corresponding author. Fax: +33 472 445 871;
russier@lasim.univ-lyon1.fr

[1] U. Kreibig and V. Vollmer, *Optical Properties of Metal Clusters* (Springer, Berlin, 1995).
[2] R. Antoine, P. F. Brevet, H. H. Girault, D. Bethell, and D. J. Schiffrin, Chem. Commun. (Cambridge) **1997**, 1901.
[3] K. Clays and A. Persoons, Phys. Rev. Lett. **66**, 2980 (1991).
[4] K. Clays and A. Persoons, Rev. Sci. Instrum. **63**, 3285 (1992).
[5] K. Clays, E. Hendrickx, M. Triest, and A. Persoons, J. Mol. Liq. **67**, 133 (1995).
[6] F. W. Vance, B. I. Lemon, and J. T. Hupp, J. Phys. Chem. B **102**, 10091 (1998).
[7] P. Galletto, P. F. Brevet, H. H. Girault, R. Antoine, and M. Broyer, Chem. Commun. (Cambridge) **1999**, 581.
[8] R. C. Johnson, J. T. Li, J. T. Hupp, and G. C. Schatz, Chem. Phys. Lett. **356**, 534 (2002).
[9] G. S. Agarwal and S. S. Jha, Solid State Commun. **41**, 499 (1982).
[10] V. L. Brudny, B. S. Mendoza, and W. L. Mochan, Phys. Rev. B **62**, 11152 (2000).
[11] J. I. Dadap, J. Shan, K. B. Eisenthal, and T. F. Heinz, Phys. Rev. Lett. **83**, 4045 (1999).
[12] E. C. Hao, G. C. Schatz, R. C. Johnson, and J. T. Hupp, J. Chem. Phys. **117**, 5963 (2002).
[13] D. Ostling, P. Stampfli, and K. H. Bennemann, Z. Phys. D: At., Mol. Clusters **28**, 169 (1993).
[14] J. Nappa, G. Revillod, I. Russier-Antoine, E. Benichou, C. Jonin, and P. F. Brevet, Phys. Rev. B **71**, 165407 (2005).
[15] I. Russier-Antoine, E. Benichou, G. Bachelier, C. Jonin, and P. F. Brevet, J. Phys. Chem. C **111**, 9044 (2007).
[16] J. Shan, J. I. Dadap, I. Stiopkin, G. A. Reider, and T. F. Heinz, Phys. Rev. A **73**, 023819 (2006).
[17] J. Nappa, I. Russier-Antoine, E. Benichou, C. Jonin, and P. F. Brevet, J. Chem. Phys. **125**, 184712 (2006).
[18] J. Nappa, I. Russier-Antoine, E. Benichou, C. Jonin, and P.-F. Brevet, Chem. Phys. Lett. **415**, 246 (2005).
[19] P. B. Johnson and R. W. Christy, Phys. Rev. B **6**, 4370 (1972).
[20] E. D. Palik, *Handbook of Optical Constants of Solids* (Academic, New York, 1985).
[21] J. Turkevich, P. C. Stevenson, and J. Hillier, Discuss. Faraday Soc. **11**, 55 (1951).
[22] J. A. Creighton, C. G. Blatchford, and M. G. Albrecht, J. Chem. Soc., Faraday Trans. 2 **75**, 790 (1979).
[23] Y. W. Cao, R. Jin, and C. A. Mirkin, J. Am. Chem. Soc. **123**, 7961 (2001).
[24] A. Henglein, J. Phys. Chem. B **104**, 2201 (2000).
[25] L. M. Lizmarzan and A. P. Philipse, J. Phys. Chem. **99**, 15120 (1995).
[26] R. H. Morriss and L. F. Collins, J. Chem. Phys. **41**, 3357 (1964).
[27] P. Mulvaney, M. Giersig, and A. Henglein, J. Phys. Chem. **97**, 7061 (1993).
[28] L. Rivas, S. Sanchez-Cortes, J. V. Garcia-Ramos, and G. Morcillo, Langmuir **16**, 9722 (2000).
[29] J.-P. Abid, J. Nappa, H. H. Girault, and P.-F. Brevet, J. Chem. Phys. **121**, 12577 (2004).
[30] S. Link, Z. L. Wang, and M. A. El-Sayed, J. Phys. Chem. B **103**, 3529 (1999).
[31] B. Rodriguez-Gonzalez, A. Sanchez-Iglesias, M. Giersig, and L. M. Liz-Marzan, Faraday Discuss. **125**, 133 (2004).

[32] G. Mie, Ann. Phys. (N.Y.) **25**, 337 (1908).
[33] K. Ripken, Z. Phys. **250**, 228 (1972).
[34] M. Gaudry, J. Lerme, E. Cottancin, M. Pellarin, J. L. Vialle, M. Broyer, B. Prevel, M. Treilleux, and P. Melinon, Phys. Rev. B **64**, 085407 (2001).
[35] G. Bachelier, Routines and numerical values for the dielectric constants of the alloyed gold-silver particles with varying composition are available at http://www-lasim.univ-lyon1.fr/spip.php?article683&lang=en
[36] P. O. Nilsson, Phys. Kondens. Mater. **11**, 1 (1970).
[37] I. Russier-Antoine, C. Jonin, J. Nappa, E. Benichou, and P. F. Brevet, J. Chem. Phys. **120**, 10748 (2004).
[38] C. F. Bohren and D. Huffman, *Absorption and Scattering of Light by Small Particles* (Wiley, New York, 1983).